11 Response of Segmented Pipelines to Wave Propagation

As noted previously, seismic wave propagation has caused damage to segmented pipelines. Damage most frequently occurs at joints, tees and elbows. The corresponding failure modes include pull-out at joints, crushing of bell-spigot joints as well as circumferential cracks due to bending. In this chapter, analytical approaches for estimating both the axial and bending strain in straight pipelines are reviewed. Observed expansion/contraction behavior of joints at elbows and connections is also presented. Finally, a somewhat special case of the influence of liquefied soil on the dynamic response of segmented pipelines is discussed.

11.1 Straight Pipelines / Tension

For a long straight run of segmented pipe, the ground strain is accommodated by a combination of pipe strain and relative axial displacement (expansion/contraction) at pipe joints. As noted by Iwamoto et al. (1984), since the overall axial stiffness for segments is typically much larger than that for the joints, the ground strain results primarily in relative displacement of the joints. As a first approximation, assuming that the pipe segment axial strain can be neglected (i.e., rigid segment) and that all joints experience the same movement, the maximum joint movement Δu is:

$$\Delta u = \varepsilon_{max} \cdot L_0 \qquad (11.1)$$

where L_0 is the pipe segment length and ε_{max} is the maximum ground strain parallel to the pipe axis, given, for example, by Equation 3.8.

For ground motion perpendicular to the pipe axis, the maximum relative rotation at pipe joints can be estimated by:

$$\Delta\theta = \kappa_g \cdot L_n \qquad (11.2)$$

where κ_g is the maximum ground curvature given, for example, by Equation 3.9. Equation 11.2 assumes that the bending strain in pipe segments is small and that all joints experience the same relative rotation

In relation to the rigid segment assumption, Wang (1979) determined the joint deformation and pipe strain using an analytical model shown in Figure 11.1, in which the joint is modeled as a linear spring with axial stiffness K_g.

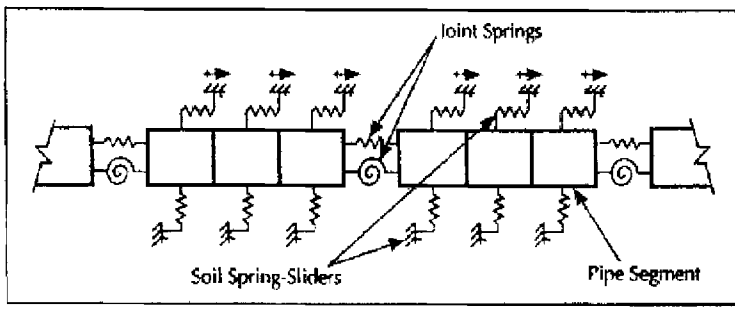

After Wang, 1979

■ Figure 11.1 Model of Segmented Pipeline

Figures 11.2 and 11.3 present the joint opening and maximum axial strain at pipe segments respectively, as a function of joint stiffness for the East West component of the 1940 El Centro event. The assumed pipe diameter is 45.7 cm (18 in), the pipe segment length is 6.1 m (20 ft), the axial soil spring has stiffness of 23.4 MPa (3400 lbs/in^2) and the propagation velocity is taken as 244 m/sec (800 ft/sec). As one expects, the joint opening is a decreasing function of the joint stiffness while the pipe strain is an increasing function of joint stiffness. That is, for a small joint stiffness, the ground deformation is accommodated primarily by joint opening

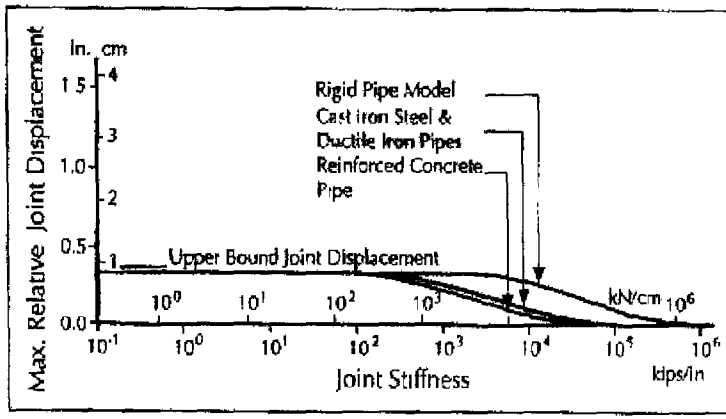

After Wang, 1979

■ **Figure 11.2 Joint Opening due to Wave Propagation vs. Joint Stiffness**

The peak ground velocity for the record used by Wang is 0.37 m/sec, and the value given by Equation 11.1 is close to the upper bound joint opening of 0.85 cm (0.32 in) in Figure 11.2.

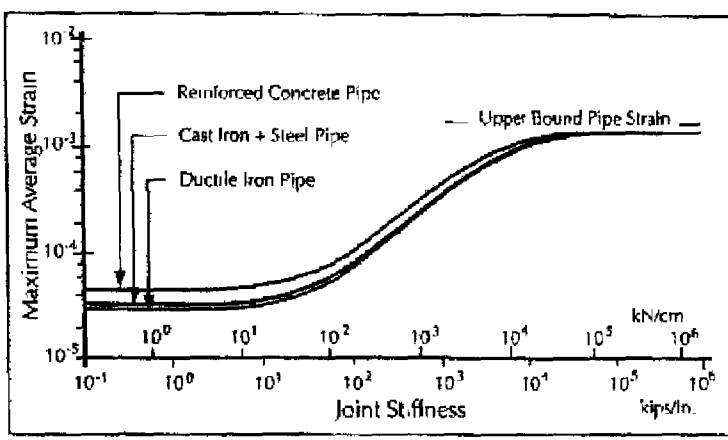

After Wang, 1979

■ **Figure 11.3 Maximum Axial Strain at Pipe Segments vs. Joint Stiffness**

The Wang model correctly captures the trend of decreasing joint opening with increasing joint stiffness. However, it assumes an equivalent linear joint stiffness while laboratory tests suggest that joint axial behavior is non-linear. Furthermore, for a given

stiffness, the relative displacement at each joint in the model is the same. That is, it does not capture the variation in displacement from joint to joint. This variation from joint to joint is considered important since even for relatively large amount of wave propagation damage, only a few joints require repair. For example, from Figure 1.3, one expects roughly 0.9 wave propagation repair per km for a peak particle velocity of 50 cm/sec. This suggests one repair for every 182 joints if the pipe segment length is 6.1 m (20 ft). That is, since it is reasonable to assume some variation in response from joint to joint, the few joints with largest response control damage as opposed to joints with "average" response. With this in mind, El Hmadi and M. O'Rourke (1990) considered a model somewhat similar to that in Figure 11.1, in which the joint properties vary from joint to joint and the soil properties vary from pipe segment to pipe segment. Specifically, a cast iron pipe with lead

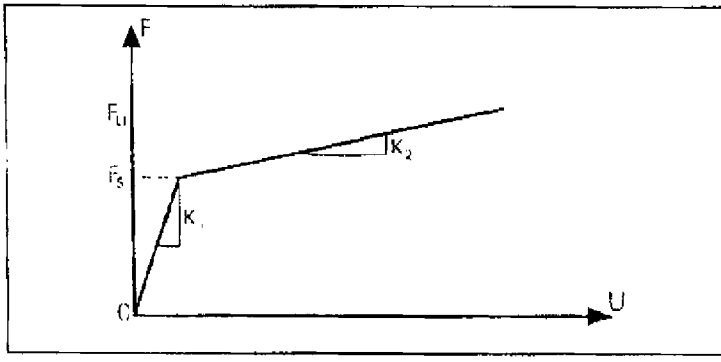

Allen El Hmadi and M. O'Rourke, 1990

■ Figure 11.4 Axial Force-Displacement Curve for a Lead Caulked Joint

caulked joints subject to tensile ground strain was considered. The assumed force-deformation relation for the joint in tension is shown in Figure 11.4. The expected variation in the joint slippage force, F_s, was based upon results by T. O'Rourke and Trautmann (1980).

A quasi-static approximation to the seismic wave propagation environment is modeled by displacing the base of the soil spring sliders in the longitudinal direction. A simplified Monte Carlo simulation technique is used to establish the characteristics of

force-displacement relationships at each joint and soil restraint along each pipe segment. Figure 11 5 shows the joint deformation as a function of ground strain for a segmented pipe with a diameter of 0 41 m (16 in).

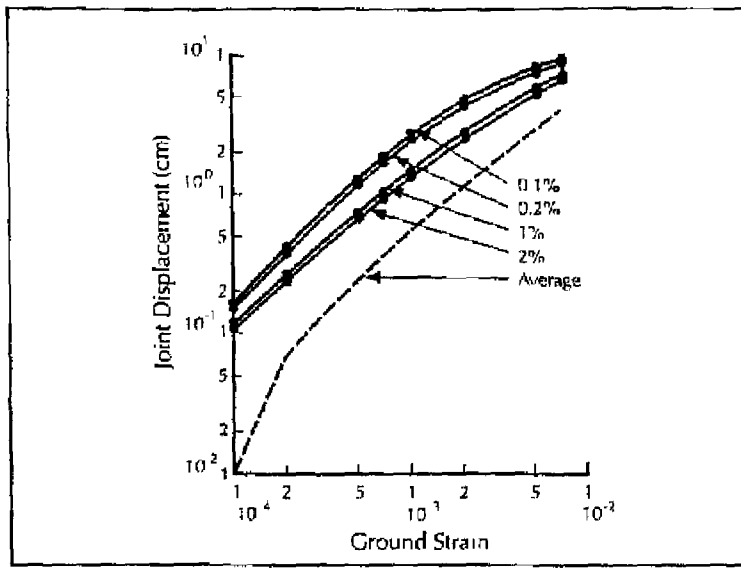

After El Hmadi and M O'Rourke, 1990

Figure 11.5 Relative Joint Displacement vs Ground Strain for 41 cm Diameter Cast Iron Pipe with Lead Caulked Joints

As shown in Figure 11 5, the average joint displacement is approximately equal to the product of the ground strain times the pipe segment length However, for the data in Figure 11.5, one in a hundred joints (1% probability of exceedence) have joint displacement about three times the average value while for the 0.1% exceedence probability (one in a thousand), the joint opening is about five times the average. This information, coupled with the probability of leakage as a function of the normalized joint opening, as shown in Figure 4.11, allows one to establish an analytically derived estimation of joint pull-out damage (repair per kilometer) as a function of ground strain. Note however, that this approach requires information, typically derived from laboratory tests, on the expected variability of joint properties.

El Hmadi and M. O'Rourke found that the variability of joint displacement was a decreasing function of pipe diameter. That is, at larger diameters, the joint displacements with 1% and 0.1% probability of exceedence were closer to the average value. This suggests that the damage ratio (repair/km) for joint pull-out in a cast iron pipe with lead caulked joints is a decreasing function of pipe diameter.

11.2 STRAIGHT PIPELINES/ COMPRESSION

Extensive damage to concrete pipelines has occurred when these elements are subject to compressive ground strain. For wave propagation resulting in compressive ground strain, the failure mode of interest is crushing (i.e., telescoping) at pipe joints. For concrete pipelines, a strength of materials model, based upon the pipe wall thickness, diameter and concrete strength, was used to establish the joint crushing force as discussed in Section 4.2.2. Figure 11.6 presents the force-displacement relationship for pipe joints subject to compressive load. This relation is based upon a series of laboratory tests on reinforced concrete cylinder pipelines (RCC) with rubber gasketed joints by Bouabid (1995).

These tests indicate that the joint behaves in a sigmoidal fashion before "lock up" (at about 0.3 inches as shown in Figure 11.6) The joint compressive displacement, Δu_{ub}, at lock-up typically ranges from 0.125 to 0.375 in (0.32-0 95 cm) with corresponding loads of 3 5 to 4.5 kips (16-20 kN).

When subject to compressive ground strain ε_g, the response of a segmented pipe is complicated by the presence of joints. Significant axial force can be transferred from joint to joint only if the contraction of the joint is Δu_{ub} (i.e., the joint is fully closed). If there are n fully closed joints in sequence and the ground strain is assumed uniform over the corresponding number of pipe segments, the pipe segment compressive strain is:

$$\varepsilon_p = \varepsilon_g - \frac{n}{n+1}\frac{\Delta u_{ult}}{L_o} \qquad (11.3)$$

where L_o is the length of pipe segment.

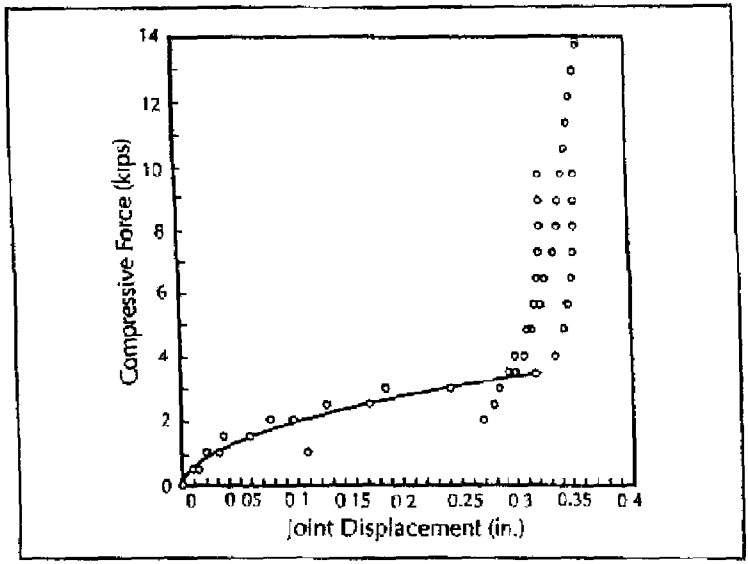

After Bouabid, 1995

■ Figure 11.6 Force-Displacement Relationship for Reinforced Concrete Cylinder Pipe Joints

The upper bound value corresponds to n=1 and

$$\varepsilon_p = \varepsilon_g - \frac{1}{2}\frac{\Delta u_{ult}}{L_o} \qquad (11.4)$$

The lower bound value corresponds to n=∞ and

$$\varepsilon_p = \varepsilon_g - \frac{\Delta u_{ult}}{L_o} \qquad (11.5)$$

For non-liquefied soil, the half-wavelength of seismic waves (corresponding to $(n+1)L_p$) is generally larger than 120 m, hence, the pipe strain is expected to be closer the lower bound value (i.e., Equation 11.5).

Using the Monte Carlo technique, M. O'Rourke and Bouabid (1996) developed fragility relations shown in Figure 11.7 for three types of concrete pipe subject to axial compression. These three pipes are 30 inch-diameter reinforced concrete cylinder pipe (30" RCC), 48 inch-diameter prestressed lined cylinder pipe (48" LCP) and 60 inch-diameter prestressed embedded cylinder pipe (60" ECP).

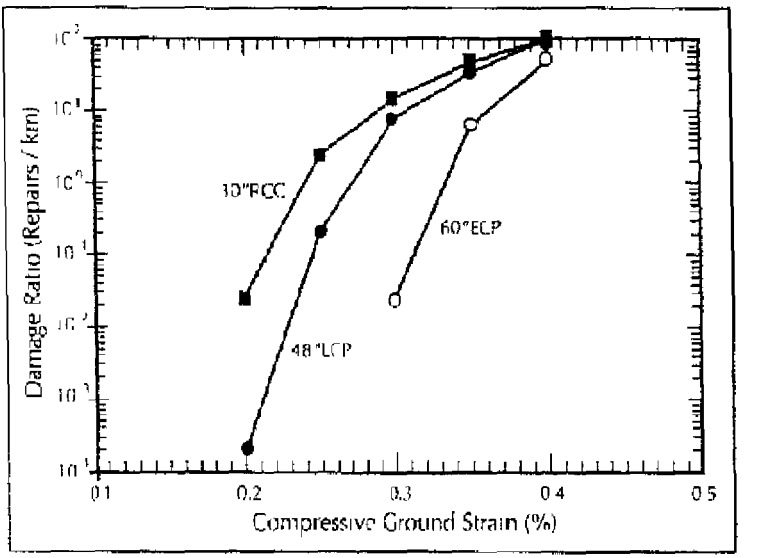

After M. O'Rourke and Bouabid, 1996

■ Figure 11.7 Analytical Fragility Curves for Concrete Pipe Subject to Compressive Ground Strain

In this case, the variation in joint crushing thresholds was based upon the cross-sectional area near the joint and an assumed normal distribution of concrete strength (mean strength of 5 ksi (34.5 MPa) and 7% coefficient of variation). During the 1985 Michoacan Earthquake, the average ground strain in the portions of Mexico City with a significant inventory of large diameter concrete pipe

was estimated by M O'Rourke and Bouabid to be about 0.0025. Note from Figure 11.7, the expected damage ratio for the 30" RCC (76 cm) pipe is about 2.4 repairs/km, but only 0.22 repairs/km for the 48" LCP (1 22 m) pipe. The estimated value for the 48" pipe, in fact, matches relatively well with the observed damage ratio of 0.20. Also most of the pipelines in this Mexico City comparison are 48 inches in diameter.

11.3 Elbows and Connections

There appear to have been relatively little analytical research on the wave propagation behavior of bends and elbows in segment pipe systems. However, measurements by Iwamoto et al. (1985) suggest that joint openings at bends and elbows are, in fact, different from those in long straight runs of pipe. For example, Figure 11.8 shows observation for three sites (Kansen, Hakusan and Shimonaga) in Japan.

For various events, the maximum expansion/contraction at an elbow is plotted versus the corresponding expansion/contraction for joints in a straight run. In some cases, the response on the elbow joint was only a tenth of that for a straight pipe joint. However, in other cases, presumably for other angles of incidence, the elbow joint response was three time larger than the straight joint response.

For pipe design purposes, it seems reasonable to use three as the amplification factor for joint openings at bends, relative to the maximum joint opening induced in corresponding straight pipelines. Iwamoto et al. (1985) also measured expansion/contraction for joints adjacent to valve boxes. As shown in Figure 11.9, the behavior is similar to that at elbows in that an amplification factor of three seems appropriate particularly for large ground strains (i.e., when the corresponding straight pipe response is larger).

Similar information from Iwamoto et al. (1985) is presented in Figure 11.10 for joints adjacent to buildings. However, in this case, the amplification factor is as large as 10

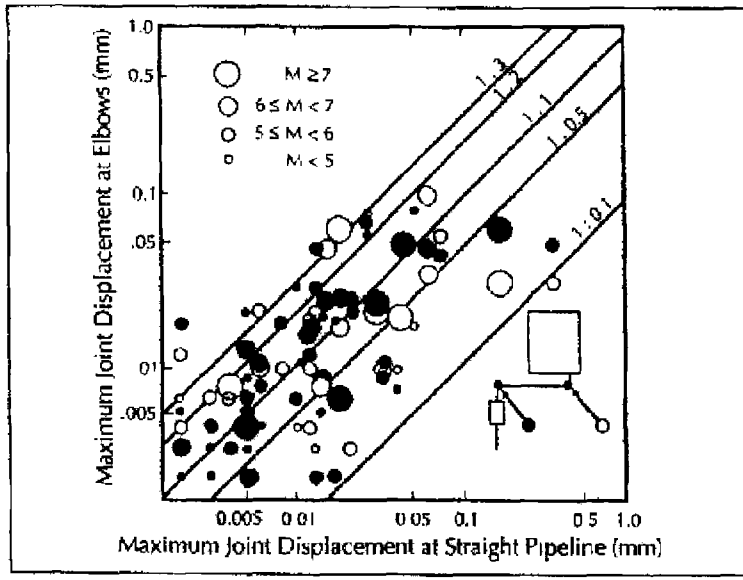

After Iwamoto et al., 1985

■ Figure 11.8 Observed Joint Displacement and Amplification Factor for Elbows

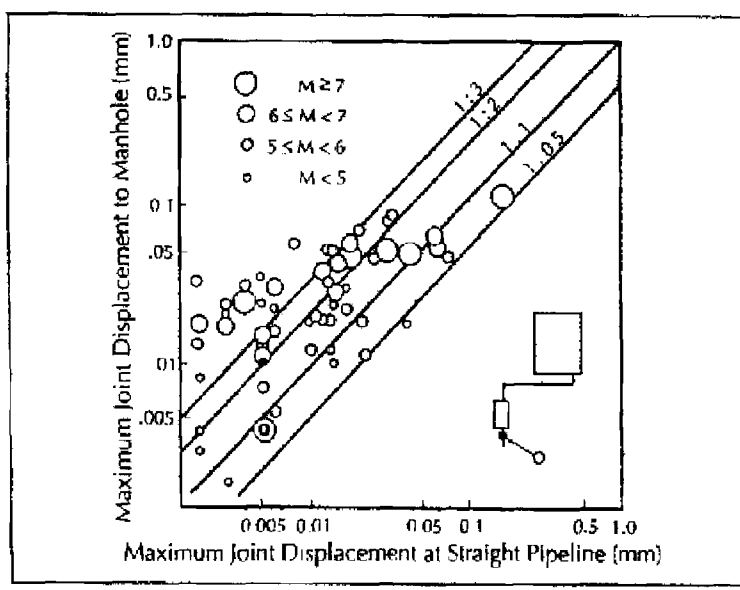

After Iwamoto et al., 1985

■ Figure 11.9 Observed Joint Displacement and Amplification Factor at Joint Adjacent to Manhole

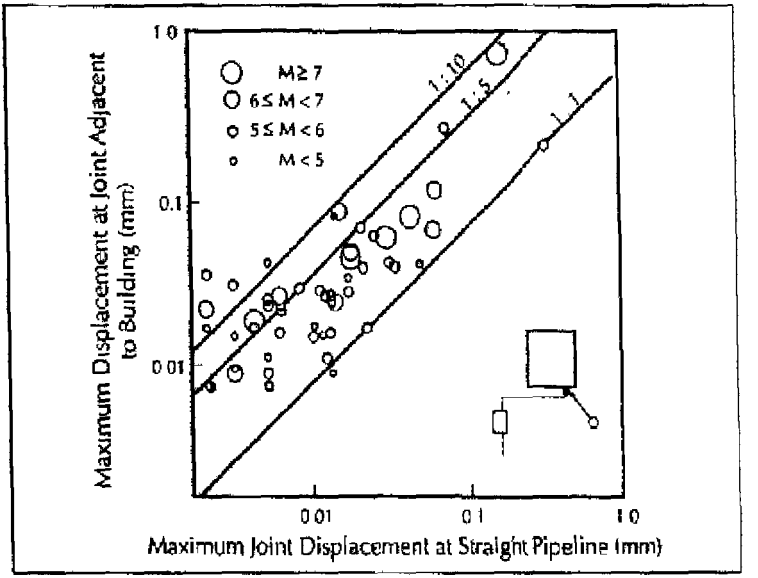

After Iwamoto et al., 1995

■ Figure 11.10 Observed Joint Displacement and Amplification Factor at Joint Adjacent to Buildings

11.4

COMPARISON AMONG APPROACHES

This section presents a comparison of three approaches for estimating joint expansion/contraction in a straight run of pipe subject to wave propagation. For the comparisor presented in Table 11.1, the peak ground velocity is taken as 0.37 m/sec and the propagation velocity near the ground surface is taken as 240 m/sec which results in a ground strain of 0.00154. The CI pipe has a diameter of about 0.44 m (specifically 0.46 m (18 in) for the Wang model, and 0.41 m (16 in) for the El Hmadi and M. O'Rourke model) and a segment length of 6.1 m. In the Wang approach, the joint axial stiffness is modeled as a linear spring, while in the El Hmadi and M. O'Rourke approach a bi-linear model is used. Specifically for a 16 in diameter with lead caulked joints, the joint stiffness K_1 and K_2 are 3.6×10^5 kN/cm (20.6 kips/in) and 26.5 kN/cm

(1.5 lbs/in), respectively. For comparison purpose, the joint opening from the Wang approach is evaluated separately assuming linear stiffness of 3.6×10^{5} kN/cm and 26.5 kN/cm, respectively.

■ Table 11.1 Comparison of Wave Propagation Response of Straight Segmented Pipelines

Item	Eqn 11.1 (Max.)	Wang (Max.)		El Hmadi & O'Rourke (Average)
		$K_j = 3.6\times10^{5}$ kN/cm	$K_j = 26.5$ kN/cm	
Ground Strain	0.00154	0.00154		0.00154
Pipe Strain	-	1.2×10^{-3}	4.0×10^{-4}	
Joint Opening (cm)	0.92	0.21	0.8	0.83 Average 2.0 1% Exceedence 3.4 0.1% Exceedence

The average joint opening from the El Hmadi and M. O'Rourke approach matches reasonably well with the results from Equation 11.1 and with the Wang approach for $K_j = 26.5$ kN/cm. However, when the initial joint stiffness of 3.6×10^{5} kN/cm is used in Wang's approach, the joint opening is much smaller and the axial strain in the pipe segments is much larger as shown in Table 11.1. This illustrates that care must be taken when attempting to model bilinear behavior (in this case the axial stiffness of CI pipe joints) with a linear model.

Based upon a joint depth (a_j in Figure 4.11) of 11.5 cm for a 16 to 18 in diameter pipe, one would not expect damage due to joint pull-out for a joint opening in the range of 0.8 to 0.92 cm since, as mentioned in Section 4.2.1, the normalized joint displacement is less than about a half ($0.92/11.5<<0.5$). However, using the El Hmadi and M. O'Rourke approach, the displacement for one in a thousand joints is 3.4 cm (normalized displacement = $3.4/11.5=0.3$) and hence, some leakage (about one in 10,000 ($1/10\times1/1000$) joints from Figure 4.11) is expected.

An advantage of the Wang approach is that an estimate of the pipe strain is provided. However, based upon the above discussion, the expected tensile strain in the segments (4.0×10^{-4} strain corresponding to 0.8 cm joint opening) is less than the yield strain for a CI pipe of about 2.0×10^{-3} from Chapter 4. Hence, although pipe strain is provided, it is unlikely that the pipe segment failure mode governs.

11.5

EFFECTS OF LIQUEFIED SOIL

The response of both segmented and continuous pipe to PGD was discussed in previous chapters. Also the uplifting response of pipe surrounded by liquefied soil was treated in Chapter 7. In this section, the somewhat special case of a buried pipeline subject to sloshing action due to liquefaction of a subsurface layer is addressed. Note that 69 breaks to segmented water mains within the Marina District during the 1989 Loma Prieta event have been attributed to this mechanism.

Laboratory experiments by Nishio et al. (1987, 1989) provided an observational basis for the phenomenon. They analyzed the dynamic response of a continuous pipeline surrounded by non-liquefied soil but underlain by a liquefied layer. Figure 11.11 shows their test set up. The pipe is 13 mm (0.51 in) in diameter and made of poly-carbonate.

The input motion at the base of the model was a sinusoidal wave with a frequency of 5 Hz and a peak acceleration of about 150 gal. Accelerations throughout the model were comparable to the base acceleration up to the time of liquefaction of the loose sand deposit. After liquefaction, the acceleration of the non-liquefied surface layer directly over the loose sand deposit was amplified by a factor of roughly 2, relative to the input acceleration. Al-

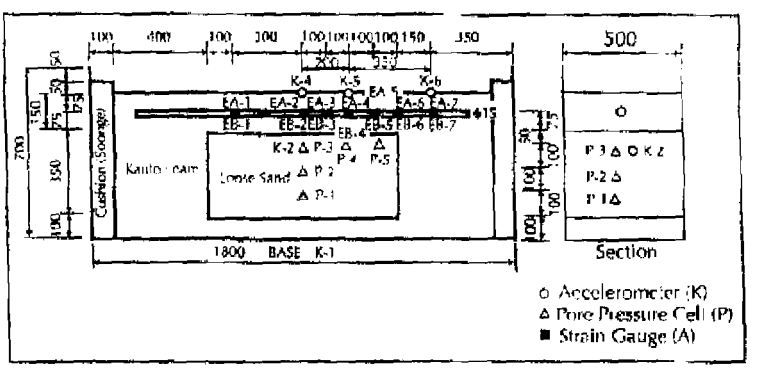

After Nishio et al. 1987

■ Figure 11.11 Configuration of Model and Locations of Gauges

though the base motion was horizontal (parallel to the pipe axis), the resulting pipe motion after liquefaction had a significant vertical component and the vertical motion was asymmetric about the center of the liquefied deposit (i.e., a sloshing type of response). Figures 11 12 and 11.13 show the distributions of pipe bending strains and axial strains at two times during the test (both after the onset of liquefaction of the subsurface deposit)

Note that the amplitude of the bending strain is roughly an order of magnitude larger than the axial strain. The axial strain is largest near the edge of the liquefaction deposit, while the bending strain is largest about a quarter of the distance from the edge. Note that a point of counter flexure exists near the center of the model, confirming the asymmetric nature of the response (e.g. left portion moving up while right portion moves down).

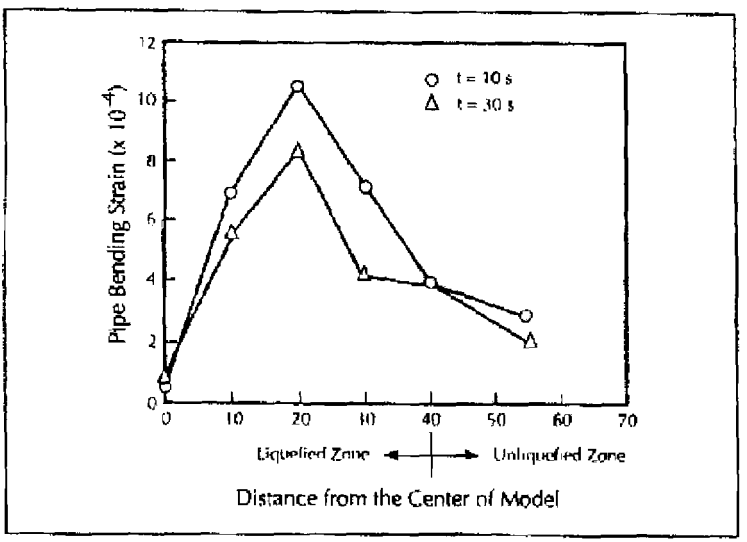

After Nishio et al., 1987

Figure 11.12 Distribution of Peak Pipe Bending Strain

Ishihara (1985) presents a relation between acceleration and thicknesses of non-liquefied surface layer and liquefied sublayer in Figure 11.14 based on the damage observation during past earthquakes. This observation suggests that for a given value of peak acceleration, the thinner non-liquefied surface layer, the more serious the damage.

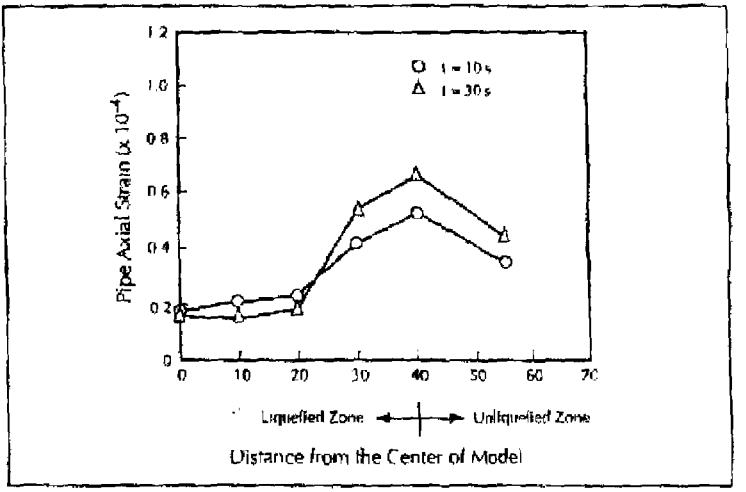

After Nishio et al., 1987

■ Figure 11.13 Distribution of Peak Pipe Axial Strain

Considering date from a wide range of earthquake and site condition, Youd and Garris (1995) evaluate and verify Ishihara's criteria. Their study suggests that the thickness bounds proposed by Ishihara appear valid for sites not susceptible to lateral spread, but not valid for site susceptible to lateral spread.

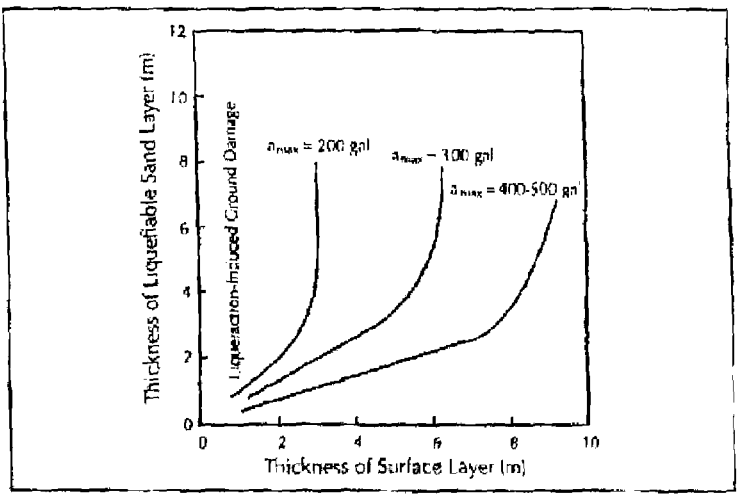

After Ishihara, 1985

■ Figure 11.14 Ishihara's Proposed Boundary Curves for Site Identification of Liquefaction Induced Damage